2006

Iridescent plumage in satin bowerbirds: structure, mechanisms and nanostructural predictors of individual variation in colour

Stéphanie M. Doucet
University of Windsor

Matthew D. Shawkey

Geoffrey E. Hill

Robert Montgomerie

Follow this and additional works at: https://scholar.uwindsor.ca/biologypub

Part of the Biology Commons

Recommended Citation

Iridescent plumage in satin bowerbirds: structure, mechanisms and nanostructural predictors of individual variation in colour

Stéphanie M. Doucet[1],*, Matthew D. Shawkey[1,†], Geoffrey E. Hill[1] and Robert Montgomerie[2]

[1]*Department of Biological Sciences, 331 Funchess Hall, Auburn University, Auburn, AL 36849, USA and*
[2]*Department of Biology, Queen's University, Kingston, ON, Canada K7L 3N6*

*Author for correspondence (e-mail: doucets@auburn.edu)

†Present address: Department of Environmental Science, Policy and Management, 137 Mulford Hall, #3114, University of California, Berkeley, CA 94720-3100, USA

Summary

Iridescence is produced by coherent scattering of light waves from alternating layers of materials of different refractive indices. In birds, iridescent colours are produced by feather barbules when light is scattered from alternating layers of keratin, melanin and air. The structure and organization of these layers, and hence the appearance of bird species with different types of plumage iridescence, varies extensively. One principal distinction between different types of iridescent colours is whether they are produced by a single pair of layers or by multiple pairs of layers. Multi-layer iridescence, such as that displayed by hummingbirds, has been relatively well characterized, but single-layer iridescence has only recently been modeled successfully. Here we use electron microscopy, spectrometry and thin-film optical modeling to investigate the glossy, ultraviolet-blue plumage colouration of adult male satin bowerbirds *Ptilonorhynchus violaceus minor*. The flattened barbules of adult males are composed of a superficial keratin layer overlying a melanin layer that is several granules thick. A thin-film model based on the thickness of the keratin layer and its two associated interfaces (air/keratin and keratin/melanin) generates predicted reflectance spectra that closely match measured spectra. In addition, hues predicted from this model are positively correlated with measured hues. As predicted from our thin-film model, measured hues shifted to shorter wavelengths at increasing angles of incidence and reflectance. Moreover, we found that individual variation in barbule nanostructure can predict measured variation in both hue and UV-chroma. Thus, we have characterized the microstructure of satin bowerbird barbules, uncovered the mechanisms responsible for producing ultraviolet iridescence in these barbules, and provided the first evidence of a nanostructural basis for individual variation in iridescent plumage colour.

Key words: feather, barbule, structural colour, iridescence, thin-film modeling, bird.

Introduction

The skin, scales, feathers, and fur of animals can be coloured by the deposition of pigments or through the physical interaction between light and nanostructural components of the integument (Fox, 1976). Both mechanisms of colour production are widespread in birds. Colours produced by feather nanostructures, termed structural colours, can be further subdivided into iridescent and non-iridescent colours. Broadly defined, iridescent structural colours change in appearance with angle of observation or illumination, while non-iridescent colours generally remain similar in appearance regardless of viewing geometry (Newton, 1730; Osorio and Ham, 2002). Both types of structural plumage colour can be produced by coherent scattering of light waves within feathers, but these two types of colouration differ in the composition and organization of their light-scattering elements (Prum, 2006).

Non-iridescent structural colours are generally produced in feather barbs. Two-dimensional Fourier analysis has revealed that quasi-ordered arrays of keratin and air within feather barbs are likely responsible for producing the turquoise, blue, violet, and ultraviolet colours found in a number of species (Prum et al., 1998, 1999, 2003; Shawkey et al., 2003; Doucet et al., 2004). By contrast, iridescent structural colours are generally produced in feather barbules (Prum, 2006), where light is scattered constructively by laminar or crystal-like arrays consisting of alternating layers of materials with different refractive indices, namely keratin, melanin and air.

Although all iridescent plumage colours are produced by the same underlying mechanism, considerable variation exists in the structure and arrangement of the alternating layers of keratin and melanin and, consequently, in the appearance of different iridescent colours. The melanin granules can be rod-

or disk-shaped, solid or hollow, and arranged in single or multiple layers (Durrer, 1986; Prum, 2006). The brilliantly coloured iridescent gorgets of many hummingbird species, for example, are produced by the coherent scattering of light from multiple, alternating layers of keratin and air-filled, disk-shaped melanin granules (Greenwalt et al., 1960; Land, 1972). The multi-coloured iridescent eye spots on the tails of male green peacocks *Pavo muticus*, by contrast, are produced by crystal-like arrays of rod-shaped melanin granules (Zi et al., 2003).

In some species, iridescence is achieved by a single pair of keratin and melanin layers. Using thin-film optical modeling based on nanostructural barbule measurements, Brink and van der Berg (2004) recently showed that the coppery-purple iridescence of the plumage of hadeda ibises *Bostrychia hagedash* is produced primarily by coherent scattering from an unusually thick (~0.8 μm) and uniform keratin cortex. The single, underlying layer of elliptical melanin platelets apparently serves mainly to define the thickness of the superficial keratin layer (Brink and van der Berg, 2004). A number of species with iridescent plumage share similarities in barbule microstructure with the hadeda ibis; that is, they contain a single superficial layer of keratin overlying either a single layer, or a solid cluster, of melanosomes (Durrer, 1986; Prum, 2006). Whether these other species produce iridescence by the same mechanistic process, however, remains to be investigated.

Here, we investigate the mechanisms of colour production in the iridescent plumage of satin bowerbirds *Ptilonorhynchus violaceus minor* Campbell 1912. Adult male satin bowerbirds have glossy, iridescent plumage that appears violet-blue to the human eye and reflects maximally at ultraviolet wavelengths (Doucet and Montgomerie, 2003b). Males exhibit delayed plumage maturation whereby juvenile males molt into a female-like green plumage each year until their seventh calendar year, when they molt into the iridescent plumage characteristic of adult males (Vellenga, 1980). Male plumage colouration may be a sexually selected indicator of quality in this species, as plumage is sexually dichromatic and variation in plumage colouration relates positively to the expression of other sexual ornaments as well as various indicators of health and condition (Doucet and Montgomerie, 2003b,c). While some studies suggest that iridescent and non-iridescent structural colouration may be condition-dependent in some species (Keyser and Hill, 1999; e.g. Doucet, 2002; McGraw et al., 2002; Hill et al., 2005), the microstructural mechanisms responsible for condition-dependent variation in structural colour remain a matter of debate (Fitzpatrick, 1998; Andersson, 1999; Prum, 1999, 2006). Shawkey et al. (2003) recently showed that in male eastern bluebirds *Sialia sialis*, intraspecific variation in non-iridescent structural plumage colouration is associated with the density and uniformity in size of nanostructural elements within the colour-producing keratin matrix of feather barbs. These findings suggest that stress-induced disruption of barb nanostructure during feather growth could be manifested in plumage colouration, thereby highlighting a mechanism whereby non-iridescent structural colours could reveal quality (Fitzpatrick, 1998; Andersson, 1999; Shawkey et al., 2003). However, the self-assembly mechanisms guiding the organization of colour-producing nanostructures in developing feathers may limit their sensitivity to environmental perturbation (Prum, 2006).

We had three objectives in this study of iridescent plumage colouration in satin bowerbirds. First, we used scanning- and transmission-electron microscopy to characterize the barbule microstructure of adult males, using barbules of juvenile males as a basis for comparison. Second, based on measurements from microscopic imaging, we used thin-film optical models to identify the mechanisms responsible for creating the iridescent ultraviolet colouration of adult males. Finally, we used spectrometry and nanostructural barbule measurements to investigate the relationship between individual variation in barbule nanostructure and iridescent plumage colour in satin bowerbirds.

Materials and methods
Feather collection

We studied satin bowerbirds *Ptilonorhynchus violaceus minor* Campbell 1912 in Mount Baldy State Forest (17°30′S, 145°30′E) near Atherton, Queensland, Australia from September to December 2000 (details in Doucet and Montgomerie, 2003b). We captured birds near active bowers using mist nets baited with blue objects. We marked individuals with a unique combination of three coloured leg bands and a stainless steel band (Australian Bird and Bat Banding Scheme). We removed 6–10 rump feathers from each individual, placed them in paper envelopes, and stored them in a cool, dry place for later analysis. We performed detailed spectrometric and microscopic analysis of feathers from 10 adult males. As a basis for comparison, we also include digital photographs and scanning- and transmission-electron images of non-iridescent green feathers of a single juvenile male from the same population.

Spectrometry

We taped feathers onto matte black cardboard for spectrometric analysis, arranging the feathers in an overlapping fashion to approximate their usual configuration on a bird's body. We measured the reflectance of these feathers using an S2000 spectrometer and deuterium tungsten-halogen light source (Ocean Optics, Dunedin, FL, USA). All measurements were taken with unpolarized light. We took readings using a bifurcated fibre-optic cable mounted in a metal-encased probe that transmitted incident light to the measurement area and reflected light to the spectrometer. The probe was mounted in a rubber sheath that excluded ambient light and maintained the probe at a fixed angle perpendicular to the feather surface, where both incident (θ_i) and reflected (θ_r) light angles=0° (see Fig. 1). This measurement geometry was used for all measurements except those specifically intended to determine
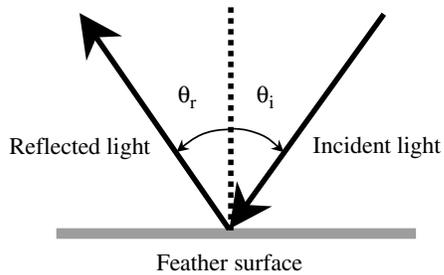
Fig. 1. Schematic representation of measurement geometries. Angles of incident (θ_i) and reflected (θ_r) light increase when moving away from a plane perpendicular to the reflective surface and are always equivalent. Reflectance measurements were taken at incident light angles of 0° (perpendicular to the feather surface) except where otherwise indicated.

the effects of varying the angle of incidence (see below). Using OOIBase32 software (Ocean Optics), we took five readings from each feather sample, with each reading comprising an average of 20 spectra measured sequentially. All measurements were expressed as percent reflectance relative to a Spectralon white standard (WS-1; Ocean Optics). We summarized our reflectance data by calculating four tristimulus colour variables to approximate three dimensions of colour: hue, brightness and spectral purity (Hailman, 1977; Montgomerie, 2006). We calculated hue as the wavelength of maximum reflectance in the bird-visible spectrum, from 300 to 700 nm (Cuthill et al., 2000; Hart, 2001). We calculated brightness as the maximum percent reflectance from 300 to 700 nm (percent reflectance at peak wavelength). We calculated two measures of spectral purity. The first, which we term 'saturation', was calculated as the quotient of the maximum reflectance minus the minimum reflectance divided by the total reflectance. This value should provide a measure of saturation that is independent of hue. The second measure of spectral purity, which we term 'UV-chroma', was calculated as the proportion of reflectance in the UV portion of the spectrum (from 300 to 400 nm). We calculated UV-chroma as it has been used previously to investigate the signal function of variation in colour in satin bowerbirds (Doucet and Montgomerie, 2003b,c).

To investigate the influence of measurement geometry on variation in reflectance, and the capacity of thin-film modeling to account for this variation, we remeasured the feathers of a single individual using separate fibre optic cables for transmitting incident and reflected light (see Fig. 1). Using an angled fibre holder (AFH-15, Avantes Inc., Boulder, CO, USA), we measured the reflectance of feathers at matching incident and reflected light angles of 15°, 30°, 45°, 60° and 75°.

Digital photography

We took digital photographs of feathers using a QImaging Micropublisher RTV 3.3 firewire camera (Burnaby, BC, Canada) connected to an Olympus SZ11 dissecting microscope (Melville, NY, USA). We collected images through an ImageJ TWAIN plugin provided by Qimaging.

Scanning electron microscopy

We mounted feathers on stubs with carbon tape (Ted Pella, Redding, CA, USA), sputter-coated them with gold on an Electron Microscopy Sciences sputter coater (Hatfield, PA, USA), and viewed them on a Zeiss DSM 930 Scanning Electron Microscope (Oberkochen, Germany).

Transmission electron microscopy

We prepared barbules from the rump feathers of 10 adult males for transmission electron microscopy (TEM) following Shawkey et al. (2003). We also embedded and sectioned the barbules of one juvenile male to allow for visual comparisons of differences in barbule ultrastructure between adults and juveniles. Using a Philips EM301 transmission electron microscope (Veeco FEI Inc, Hillsboro, OR, USA), we took micrographs of cross-sections of feather barbules at 2500× magnification. To calibrate the images, we took micrographs of a waffle-pattern diffraction grating (Ted Pella, Redding, CA, USA), accurate to 1 nm ±5% at the same magnification. We scanned these micrographs at 400 d.p.i. using an Epson Perfection 1240U flatbed scanner and used NIH Image v 1.62 (available for download at http://rsb.info.nih.gov/nih-image/index.html) to measure six nanostructural variables (Fig. 3E, Table 1). (1) We measured the thickness of the keratin cortex and (2) the thickness of the outer melanin layer at six evenly spaced points surrounding each barbule. We defined the outer melanin layer as the layer including all melanin granules that, beginning at the cortex, were contiguous with other melanin granules. (3) We also counted the number of melanin granules encountered at each of the six measurement locations of the thickness of the outer melanin layer, so that we could calculate the mean number of melanin granules comprising the melanin layer. (4) We measured the thickness of each barbule at three evenly spaced locations along the width of the barbule. (5) To estimate the percentage of melanin in the outer layer, we used Carnoy (available at http://www.kuleuven.ac.be/bio/sys/carnoy/) to measure the

Table 1. *Nanostructural measurements from transmission electron microscopy images of iridescent barbule components from rump feathers of adult male satin bowerbirds*

Variable	Mean ± s.e.m. (N=10)
Cortex thickness (nm)	163.4±1.8
Thickness of outer melanin layer (nm)	1231.9±50.4
Number of melanin granules in outer layer	3.2±0.1
Percentage of melanin in outer layer (%)	82.5±2.6
Percentage of melanin in inner layer (%)	27.8±1.2
Barbule thickness (μm)	5.6±0.1

Measurements are based on six measurements per barbule and five barbules per individual.

cross-sectional area of melanin in the outer layer. We divided this value by the total cross-sectional area of the outer layer to obtain a measure of the percentage of melanin in the outer layer. (6) Using a similar approach, we obtained a measure of the percentage of melanin in the center of barbules, beneath the outer layer. For simplicity, we refer to this latter measurement as the percentage of melanin in the inner layer (Table 1). We measured five barbules for each adult male and used mean values in our analyses.

Thin-film optical modeling

We used a standard transfer matrix thin-film optical model (Jellison, 1993) to determine how iridescent colour is produced in satin bowerbirds (see model details in Appendix). We used this model to predict the reflectance spectra of feathers from the thickness and optical properties of keratin and melanin layers, allowing us to evaluate the relative importance of these layers in determining reflectance characteristics and providing insight into how variation in each might affect colouration. We used previously published, empirically estimated refractive indices of air (n=1.00), keratin (n=1.56) and eumelanin (n=2.00) (Land, 1972; Brink and van der Berg, 2004), estimated lower limit extinction coefficients for keratin (k=0.03) and eumelanin (k=0.6) (Brink and van der Berg, 2004), as well as angles of incidence and reflectance matching those of our measured spectra in all of our calculations. Although we used unpolarized light for our spectral measurement, the Appendix includes formulae for both s- and p-polarized light. At smaller angles of incidence, models calculated from s- and p-polarized light predicted very similar reflectance spectra. However, Brewster angles ranging between 38° and 57° (calculated as $\tan^{-1}(n_2/n_1)$, where n_2 and n_1 are the refractive indices of the respective media) predict that the p-component will largely disappear at initial angles of incidence greater than 40°. Because of this effect, and because reflectance spectra predicted by s- and p-polarization were similar up to initial angles of incidence of 40°, we present only model results from s-polarization.

We created four hypothetical thin-film reflectance models, using all possible two- and three-beam combinations for the upper surface of the barbule (Fig. 2). Model 1 included all three interfaces of materials of different refractive indices (air/keratin, keratin/melanin, melanin/keratin) and the thicknesses of the keratin and melanin layers. Model 2 included only the outer two interfaces (air/keratin, keratin/melanin) and the thickness of the keratin layer. Model 3 included only the air/keratin and melanin/keratin interfaces, and the thickness of the melanin layer. Model 4 included only the inner two interfaces (keratin/melanin, melanin keratin) and the thickness of the melanin layer. We visually compared the spectra produced by these models to measured reflectance spectra from the feathers. For the model with the best predictive ability, we compared hues generated by the model to measured hues across individual males.
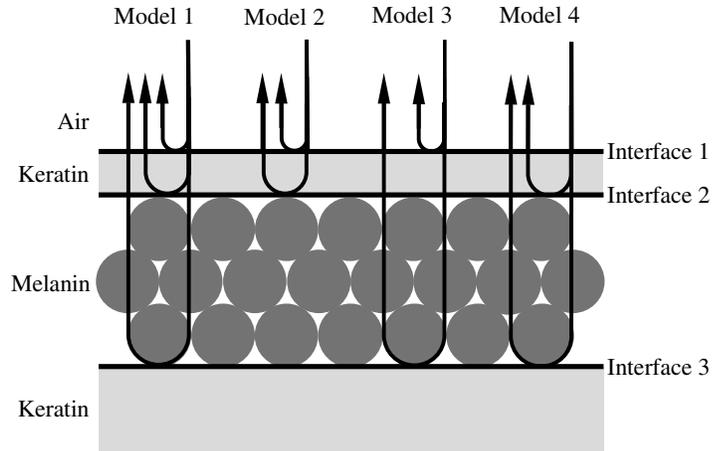

Fig. 2. Schematic representation of the four different thin-film models investigated in this study. Curved arrows represent beams of light. The models represent all possible combinations of layers and interfaces for the upper surface of the iridescent barbules of adult male satin bowerbirds.

Statistical analyses

Descriptive statistics are reported as means ± standard error (s.e.m.). To determine whether variation in barbule microstructure could predict variation in colour, we constructed stepwise regression models using a backward elimination procedure. We constructed three models, each with a different colour variable (hue, UV-chroma and brightness) as the independent variable. In each model, we used cortex thickness, the thickness of the outer melanin layer, the percentage of melanin in the outer layer, the percentage of melanin in the inner layer, and barbule thickness as potential predictor variables. Probabilities to leave the model were set at 0.05.

Results
Barbule microstructure

The iridescent, ultraviolet-blue colour of adult male satin bowerbirds is produced by feather barbules, whereas the green colour of young males is produced by feather barbs (Fig. 3A,B). In adult males, the numerous barbules are elongated, flattened and twisted at the base so that they overlay the barbs and are parallel to the feather surface (Fig. 3C). By contrast, the barbules of juvenile males are short, more cylindrical and sparsely distributed (Fig. 3D). Cross-sections of the iridescent barbules of adult males revealed a uniform and relatively thin keratin cortex (163.4±1.8 nm), beneath which lay a thick outer layer of melanin (1231.9±50.4 nm) comprising 3.2±0.1 melanin granules, on average (Fig. 3E,G; Tables 1, 2). Most barbules also had some melanin granules in their centres, though these were not distributed in a contiguous layer and were found at much lower densities (Fig. 3E; Table 1). The melanin granules in the barbules of juvenile males were evenly distributed rather than concentrated in a discrete outer layer (Fig. 3F).
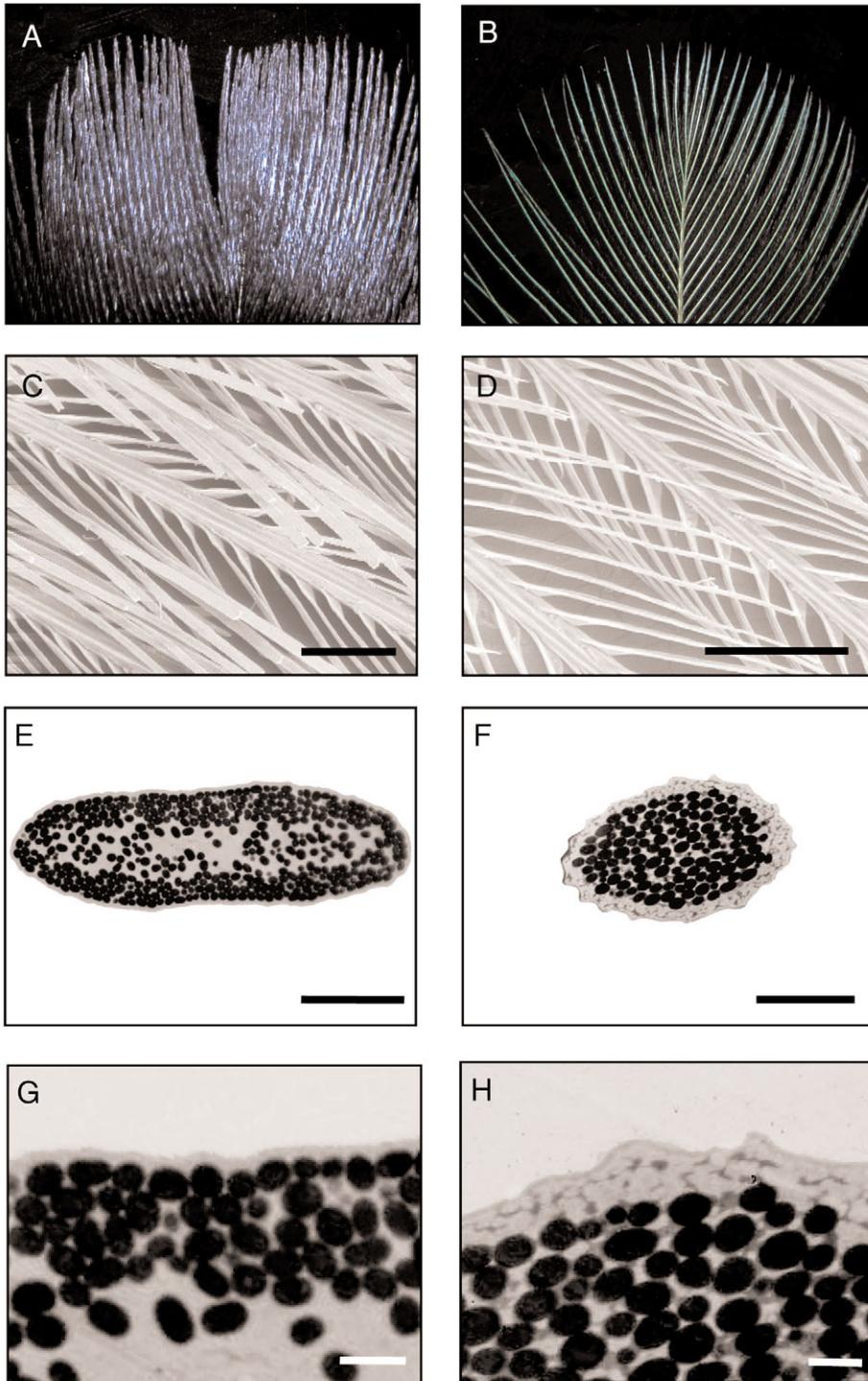
Fig. 3. Comparison of the feathers of adult (A,C,E,G) and juvenile (B,D,F,H) male satin bowerbirds. (A,B) Photographs of feathers; (C,D) scanning electron micrographs of barbs and barbules; (E–H) transmission electron micrographs of barbule cross-sections. In transmission electron micrographs, the dark ovals are melanin granules and the grey areas are keratin. Scale bars, 200 μm (C,D), 5 μm (E,F), 800 nm (G,H). Note that the scanning electron micrograph shown in C was taken at the proximal end of feather barbs to allow visualization of the twisting and flattening of barbules. The distal ends of feather barbs are much more densely covered with barbules.

Moreover, the barbules of juvenile males were smaller and narrower than those of adult males and had a thick, irregular cortex (Fig. 3D,F,H).

Thin-film optical modeling

Model 2 generated predicted reflectance spectra that closely matched measured spectra from bowerbird feathers (Fig. 4). This model incorporated only the thickness of the keratin cortex and its associated interfaces (air/keratin and keratin/melanin).

Spectra predicted from Model 2, despite exhibiting slightly narrower and lower reflectance peaks, were strikingly similar to measured spectra (Fig. 4). The other three models, which included all other possible combinations of the three layers (air, keratin and melanin) and their associated interfaces, generated predicted reflectance spectra that poorly matched measured spectra (Fig. 4). Considerable changes in the values of the extinction coefficients and refractive indices of the different layers did not substantially improve the fit of these models to

Table 2. *Cortex thickness from transmission electron microscopy images of iridescent barbule components from rump feathers of adult male satin bowerbirds*

Individual	Cortex thickness (nm)
1	160.3±2.9
2	160.8±5.1
3	168.2±19.9
4	154.1±2.7
5	165.0±5.7
6	166.9±2.5
7	157.6±6.1
8	164.2±2.4
9	163.3±8.4
10	173.9±5.0

Values are means ± s.e.m., based on six measurements per barbule and five barbules per individual.

predicted spectra (M. D. Shawkey, unpublished data). Moreover, modifying the extinction coefficients of keratin and melanin (Fig. 5A) or the refractive index of melanin (Fig. 5B) did not substantially change the predictive ability of Model 2. These results strongly suggest that scattering of light by the outer cortex layer alone is sufficient to cause the observed colour of adult male satin bowerbird feathers, regardless of minor fluctuations in the optical properties of the scattering elements. If we expand our thin-film model matrices to include infrared wavelengths, Model 2 predicts a fundamental peak at 1325 nm (Fig. 6), well beyond the bird-visible range. Thus, the peak of reflectance within bird-visible wavelengths is actually a second order harmonic of the fundamental peak. Models 1, 3, and 4 predict fundamental peaks at 855 nm, <300 nm and 1311 nm, respectively.

In Model 2, the only parameter likely to vary between individuals was cortex thickness, as the only other variables incorporated in the model – the refractive indices and extinction coefficients of the different layers – are expected to remain constant across individuals. Changing cortex thickness in the model resulted in reflectance spectra with identical shapes that were shifted to longer or shorter wavelengths when cortex thickness was increased or decreased, respectively. We calculated predicted hues (wavelength at maximum reflectance) from reflectance spectra generated by Model 2 based on each individual's mean measured cortex thickness (Table 2) and compared these to measured hues for those individuals (Fig. 7). Both predicted and measured hues varied linearly with cortex thickness (Fig. 7), and there was a significant positive correlation between predicted and measured hues ($r=0.64$, $N=10$, $P=0.04$).

We also investigated the effect of varying the angle of incidence on the shape of reflectance spectra. Hue decreased linearly with increasing angles of incidence ($r=-0.95$, $N=6$ angles, $P=0.003$), whereas brightness decreased at small angles of incidence and increased at large angles of incidence (Fig. 8). The increasing brightness at larger angles of incidence was largely caused by non-selective specular reflectance (glare), as
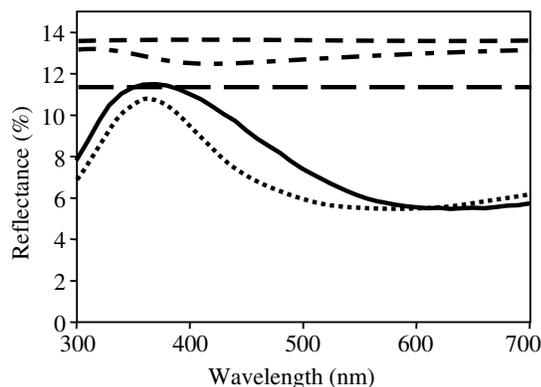

Fig. 4. Comparison of adult male satin bowerbird reflectance spectra, either measured using a spectrometer (solid lines) or predicted from thin-film optical models (broken and dotted lines). Predicted spectra are modeled based on measurements of barbule nanostructure from the individual whose measured spectrum is shown. Model 2 (dotted line) closely predicted measured spectra (solid line). By contrast, Models 1 (dashes and dots), 3 (short dashes), and 4 (long dashes) were poor predictors of measured spectra.
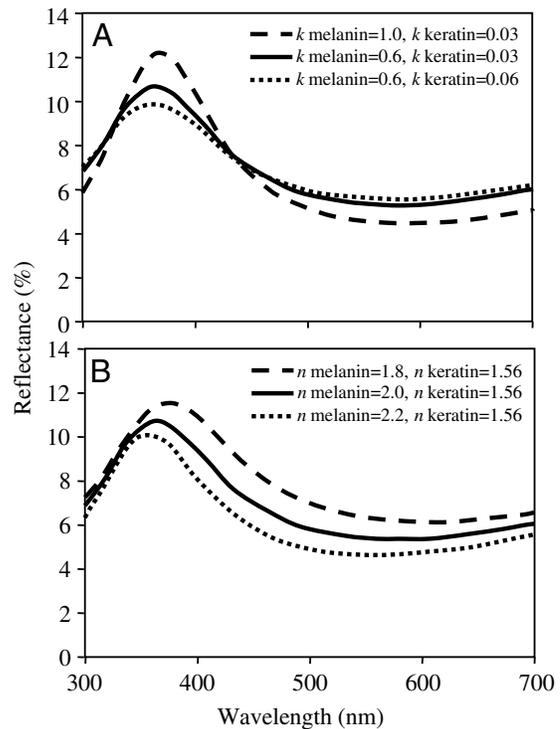

Fig. 5. Graphical representation of the effect of changing various parameters on the predictive ability of thin-film Model 2. (A,B) The solid line shows Model 2 calculated from the variables as described in the text (extinction coefficient k of keratin=0.03, melanin=0.6; refractive index n of keratin=1.56, melanin=2.0). (A) The effects of increasing k of keratin to 0.06 (dotted line) and melanin to 1.0 (broken line). (B) The effects of increasing n of melanin to 2.2 (dotted line) and decreasing n of melanin to 1.8 (broken line).
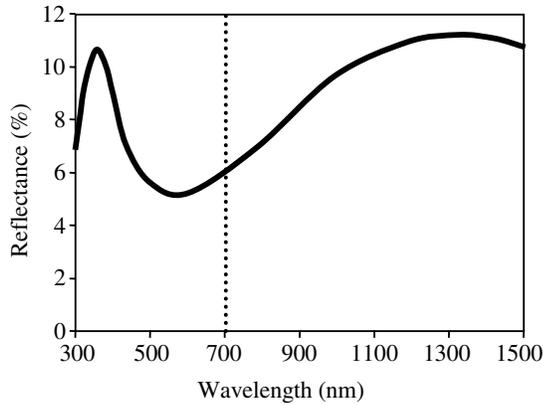
Fig. 6. Reflectance of adult male satin bowerbird barbules predicted by Model 2. The dotted line separates bird-visible wavelengths (300–700 nm) from near-infrared wavelengths (700–1400 nm). The bird-visible reflectance peak is a second-order harmonic of the fundamental peak in the near-infrared.

Fig. 8. Changes in brightness (diamonds) and saturation (circles) of adult male bowerbird feathers measured at different angles of incidence.
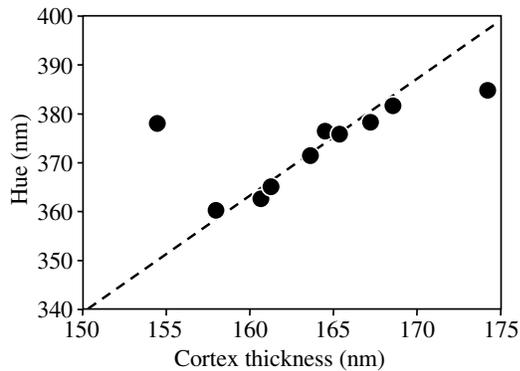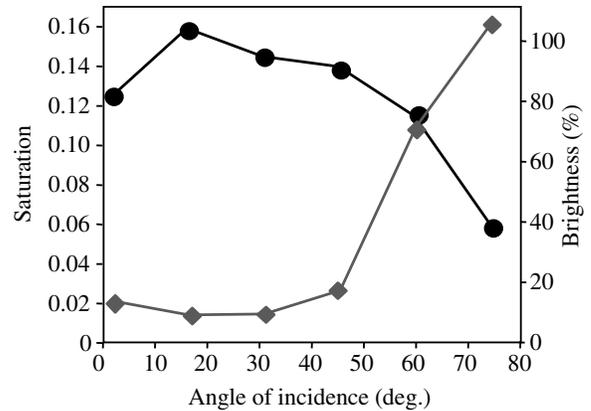

Fig. 7. Relation between cortex thickness and hues predicted from thin-film optical theory using Model 2 (broken line) and hues measured with a reflectance spectrometer (solid circles) for the iridescent rump feathers of adult male satin bowerbirds.
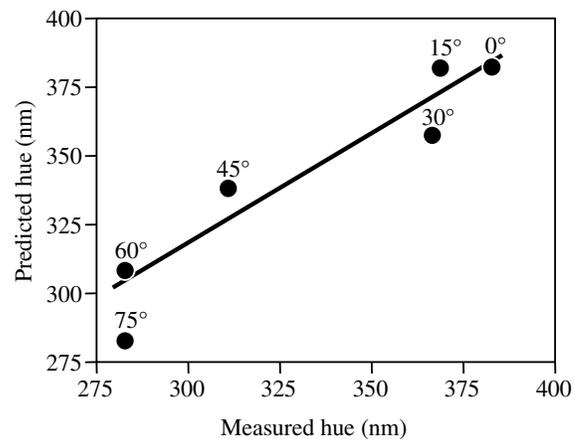

Fig. 9. Relationship between hues predicted from thin-film optical theory (Model 2) and hues measured with a reflectance spectrometer for the iridescent rump feathers of adult male satin bowerbirds measured at six different angles of incidence (angles shown above symbols).

evidenced by the decrease in saturation at those same angles (Fig. 8). We compared hues measured at different angles of incidence with hues predicted from Model 2 at those same angles and found a significant positive relationship between measured and predicted hues (Fig. 9, $r=0.96$, $N=6$ angles, $P=0.002$).

Microstructure and individual variation in colour

Cortex thickness significantly predicted hue, such that males with thicker barbule cortexes had plumage reflectance that peaked at longer wavelengths (Table 3). The percentage of melanin in both the outer and inner layers significantly predicted UV-chroma, such that individuals with greater

Table 3. *Nanostructural predictors of plumage colour variables in adult male satin bowerbirds from multiple regression models*

Colour variable	Predictors	R^2	β	d.f.	P
Hue	Cortex thickness	0.41	0.64	1,8	0.04
UV chroma	Whole model	0.65		2,7	0.03
	Percentage of melanin in inner layer	0.36	1.0	1,8	0.009
	Percentage of melanin in outer layer	0.29	0.69	1,8	0.05
Brightness	No significant predictors				

R^2, coefficient of multiple determination; β, standardized partial regression coefficient; d.f., degrees of freedom; P, probability values. Only significant ($P \leq 0.05$) predictors are shown.

densities of melanin in their barbules had plumage that reflected proportionally more in the UV (Table 3). None of the nanostructural variables significantly predicted plumage brightness (Table 3; all $P>0.26$).

Discussion

The iridescent barbules of adult male satin bowerbirds are composed of a superficial keratin cortex overlying a discrete layer of solid melanin granules. This outer layer of melanin surrounds the center of the barbule, which is composed of sparsely distributed melanin granules embedded in keratin. Using thin-film optical modeling, we show that the keratin cortex layer is largely responsible for producing ultraviolet, iridescent colouration in this species. Moreover, we show that individual variation in barbule nanostructure can predict measured differences in iridescent plumage colouration. Our findings thus contribute to a growing understanding of the mechanistic basis for glossy iridescence and identify aspects of barbule microstructure that could potentially contribute to quality signaling.

Compared with the non-iridescent barbules of juvenile males, the iridescent barbules of adult male satin bowerbirds are enlarged, elongated, flattened and twisted at the base so that the flattened surface of the barbules is parallel with the surface of the feathers. Moreover, the barbules of adult males have a thin cortex of uniform thickness whereas those of juveniles have a thick, irregular cortex. These differences in barbule microstructure highlight the remarkable change in appearance that accompanies sexual maturation in this species. Olive-green plumage can be caused by the deposition of carotenoid pigments in the barbs and melanin pigments in the barbules, or by the combination of a blue-producing keratin matrix and yellow carotenoid pigments in the barb (Dyck, 1978). Because the barbs of juvenile male satin bowerbirds have a greenish appearance, the latter mechanism is likely responsible (Dyck, 1978), though this hypothesis requires further confirmation. Thus, when molting from their juvenile to adult plumages, males switch to an entirely different colour production mechanism, from a non-iridescent green colour produced in the barbs to an iridescent ultraviolet colour produced in the barbules.

Specialized barbule morphology, as exemplified by the flattened, twisted barbules of adult male satin bowerbirds, is widespread among birds with iridescent colour and likely plays a role in enhancing the efficiency of iridescent colour displays (Osorio and Ham, 2002; Brink and van der Berg, 2004; Prum, 2006). In satin bowerbirds, males build avenue-shaped bowers of small twigs. Males perform courtship displays on a decorated platform directly in front the bower avenue, and females observe displaying males from within these avenue walls (Borgia, 1986). Thus, females necessarily observe displaying males from a fixed viewing geometry. In our rainforest population, males build their bowers where tree falls or human disturbance have created a canopy gap, orienting their bowers such that they face away from these gaps and upslope (Doucet and Montgomerie, 2003a). This configuration maximizes the frontal illumination of males during courtship displays. According to our spectral measurements, this viewing geometry, which corresponds to small angles of incident and reflected light, would result in highly saturated and relatively bright male plumage reflectance for body regions facing the female. Females would also observe occasional bright flashes of reflectance (specular highlights or glare) as the males perform their ritualized courtship displays. Most importantly, this viewing geometry ensures that male plumage will always show some interference-based reflectance. By contrast, increasing the angle of incidence without simultaneously increasing the angle of reflected light (as would occur if male bowerbirds were illuminated from above or behind) results in increasingly dull and unsaturated reflectance spectra that are indistinguishable from black at angles of incidence $>45°$ (S. M. Doucet, unpublished data). Similarly, the association of the bower location with a canopy gap likely enhances the plumage display, as males often appear black rather than blue under the cover of dense rainforest canopy (S. M. Doucet, personal observation). Among other species with iridescent colouration, barbules are tilted away from the exposed surface of the feather such that different combinations of illumination and viewing angles result in the brightest or most saturated reflectance (Osorio and Ham, 2002). The crown feathers of the magnificent hummingbird *Eugenes fulgens*, for example, have barbules that are tilted at $42°$ away from the surface of the feather, resulting in the brightest and most saturated reflectance when illuminated from above and viewed from directly in front of a displaying bird (Osorio and Ham, 2002). A comparative investigation of barbule structure and display orientation among iridescent species would provide fascinating insights into the strength of selection for behavioural and morphological modifications that enhance iridescent colour displays.

Thin-film Model 2, which incorporated only properties of the keratin cortex and its associated interfaces, predicted reflectance spectra that closely matched measured spectra. The other three models predicted reflectance spectra that were much flatter, slightly brighter and, in all but one case, of a very different shape, than measured spectra. Although the refractive indices of keratin and air are well established (Land, 1972), the refractive index of eumelanin has only recently been empirically determined (Brink and van der Berg, 2004), and the extinction coefficients of keratin and melanin are lower-limit estimates based on a single study (Brink and van der Berg, 2004). Our data show, however, that the predictive abilities of the other models cannot be substantially improved by changing these variables, and that the predictions of Model 2 are relatively robust to such changes. The melanin layer of satin bowerbird barbules is so thick and densely packed that it likely absorbs most of the light that reaches it and thus plays a limited role in creating iridescence, serving primarily to delineate the thickness of the cortex. This likely explains why the other three models, all of which included scattering from the melanin layer, could not accurately predict bowerbird

reflectance spectra. Correspondingly, models incorporating layers below the outer melanin layer also failed to predict satin bowerbird reflectance spectra (M. D. Shawkey, unpublished data). Our findings therefore suggest that, as in the hadeda ibis (Brink and van der Berg, 2004), the iridescent colour of adult male satin bowerbirds is produced primarily by constructive interference of light within the barbule cortex. The interference of light predicted by the other models, particularly Model 1, may subtly influence the shape of reflectance spectra, but they are unlikely to contribute to variation in hue.

Measured reflectance spectra were slightly brighter and less saturated than those predicted by the best model (Model 2). However, this model assumed idealized reflectance from a single barbule, whereas we measured reflectance from several barbules at once. One possible explanation is that the slight discrepancy between the curves may have been caused by subtle variation in the orientation of the reflecting surface of barbules on the feathers that we measured. Because changes in measurement geometry lead to concurrent changes in hue, brightness and saturation, subtle variation in the orientation of barbules might explain the broader and brighter peaks of measured spectra. Our model also makes the assumption that the melanin layer is uniform. However, keratin fills the small spaces between melanin granules. This heterogeneity of the melanin layer may result in the dephasing of light waves entering this layer, producing incoherent scattering that would decrease saturation and broaden reflectance peaks. This interpretation receives indirect support from the observation that individuals with more densely packed melanin granules exhibit plumage reflectance with greater UV chroma (see below).

Model 2 predicted hue closely, often within 10 nm of measured hue. Indeed, there was a significant positive correlation between hues predicted from the model, based on each individual's cortex thickness, and hues calculated from reflectance spectra. Two individuals deviated noticeably from the hues predicted by their cortex thickness. Such a discrepancy could occur if the barbules we sectioned were not representative of typical barbules in that individual, if the barbule cross-sections were not exactly perpendicular, or if the barbules were sectioned near the proximal end, which exhibits reduced iridescence. Increasing the angle of incidence (and reflectance) of our measurements resulted in a significant, linear decrease in hue. Model 2 predicted a similar decrease in hue with increasing angle of incidence, as shown by the positive association between measured and predicted hues at 6 different angles of incidence. Such a shift toward shorter-wavelength hues is expected from thin-film optical theory, as changing the angle of incidence effectively changes the thickness of the thin-film layers (Land, 1972). Not surprisingly, similar shifts to shorter wavelengths with increasing angles of incidence have been reported in a number of species with iridescent plumage colouration (Cuthill et al., 1999; Osorio and Ham, 2002; Brink and van der Berg, 2004).

Model 2 predicts a fundamental peak of reflectance at near-infrared wavelengths, suggesting that the peak of reflectance that we measured is a second-order harmonic of this near-infrared peak. It should be noted, however, that the fundamental peak in the infrared is unlikely to play any role in signaling, as it is beyond wavelengths that can be detected by birds (Cuthill et al., 2000; Hart, 2001).

Although the structural colouration of satin bowerbirds and hadeda ibises appears to be produced by the same functional, one-layer mechanism, the resulting reflectance spectra, and hence appearance of these birds, is remarkably different. We have shown that this difference is caused solely by the difference in cortex thickness between the species. As is true of all thin-film optical structures (Vačíšek, 1960), adjustment of the thickness of a material with particular refractive and absorptive properties creates strikingly different colours. The apparent simplicity of this mechanism for variation suggests that iridescent colours, once evolved, may diverge rapidly during speciation (Prum, 2006). Indeed, a recent study suggests that the interspecific diversity of iridescent colours among closely related cowbird species in the genus *Molothrus* (from glossy violet to green) evolved primarily through changes in cortex thickness, following a shift from matte black to iridescent through the rearrangement and loss of melanin granules (M. D. Shawkey, M. E. Hauber, L. K. Estep, and G. E. Hill, manuscript submitted for publication). Thus, subtle modifications of this simple, single-layer mechanism have enabled the evolution of myriad colours.

Whether and how iridescent colours might be used as condition-dependent sexual signals remain controversial (Andersson, 1999; Osorio and Ham, 2002; Prum, 2006). An important first step to addressing these questions involves identification of the microstructural mechanisms responsible for causing intraspecific variation in colour (Shawkey et al., 2003; Shawkey and Hill, 2005; Hill et al., 2005). As expected from our thin-film optical models, variation in hue was significantly predicted by cortex thickness. Additionally, UV-chroma was significantly predicted by the percentage of melanin in both the outer and inner layers of the barbule. When incident light penetrates beyond colour-producing nanostructures (in this case, the keratin cortex), the tissues below these nanostructures can scatter light incoherently, reducing the overall saturation of the colour (Prum, 2006). Presumably, an increase in the density of melanin reduces the amount of incident light that can penetrate beyond the cortex, thereby reducing the amount of incoherent scattering and increasing the UV-chroma of the colour. We have thus identified two aspects of barbule microstructure that predict intraspecific variation in iridescent colour. If these microstructural variables are associated with genetic quality, are sensitive to physiological stress during feather development, or both, they could represent a means by which iridescent structural colours may honestly signal quality in satin bowerbirds (Doucet and Montgomerie, 2003b) and other species. None of our measures of barbule microstructure significantly predicted brightness. Identifying a relationship between barbule microstructure and brightness may require

the measurement of reflectance from individual barbules. Alternatively, brightness might relate to larger-scale factors (Shawkey et al., 2003), such as the number of coloured barbules on feathers or the condition of these barbules, which could in turn be influenced by barbule loss, breakage or abrasion. Hence, iridescent colouration could also be informative if there is individual variation in susceptibility to feather damage (Osorio and Ham, 2002). Clearly, more research is needed in this area. Convincing evidence of direct condition-dependence of structural colouration would require an experimental demonstration of the effects of stress during feather growth on both microstructure and colour.

Our results have implications for investigations of iridescent plumage colouration at both proximate and ultimate levels. At a proximate level, our study complements and extends other recent work on the physical mechanisms of iridescent colour production and lays a methodological foundation for the elucidation of the mechanistic basis for iridescence in other taxa. At an ultimate level, our study provides tantalizing evidence that at least some of the tremendous diversity of iridescent colours in birds can evolve through relatively minor variation in feather nanostructure. Future studies should use large-scale phylogenetic analyses to explicitly examine the evolution of structural colour mechanisms. Furthermore, we have identified nanostructural mechanisms responsible for creating intraspecific variation in iridescent colour, providing further insight into how these colours might evolve as signals of individual quality.

Appendix

Following Jellison (1993), we treated each interface as matrices of the form:

$$I_{j,s} = \begin{bmatrix} 1 & r_{j,s} \\ r_{j,s} & 1 \end{bmatrix} \quad I_{j,p} = \begin{bmatrix} 1 & r_{j,p} \\ r_{j,p} & 1 \end{bmatrix}, \quad (1)$$

where

$$r_{j,s} = (\tilde{n}_j \cos\phi_{j-1} - \tilde{n}_{j-1} \cos\phi_j) / (\tilde{n}_j \cos\phi_{j-1} + \tilde{n}_{j-1} \cos\phi_j),$$

$$r_{j,p} = (\tilde{n}_{j-1} \cos\phi_{j-1} - \tilde{n}_j \cos\phi_j) / (\tilde{n}_{j-1} \cos\phi_{j-1} + \tilde{n}_j \cos\phi_j) \cdot \quad (2)$$

s indicates s polarization and p indicates p polarization. $\tilde{n}_j$ and $\tilde{n}_{j-1}$ are the complex refractive indices ($\tilde{n}=n-ik$, where n=real refractive index and k=extinction coefficient) of the layer under consideration and the layer above it, respectively. ϕ_j and ϕ_{j-1} are the complex angles of incidence, calculated using Snell's law: $\tilde{n}_0 \sin\phi_0 = \tilde{n}_j \sin\phi_j$.

The transfer matrix incorporated the thickness of the *j*th layer:

$$L_j = \begin{bmatrix} \exp(ib_j) & 0 \\ 0 & \exp(-ib_j) \end{bmatrix}. \quad (3)$$

$b_j=(2\pi d_j \tilde{n}_j \cos\phi_j)/\lambda$, where d_j is the thickness of the layer, and λ is the wavelength of light.

The total scattering matrix is then given by:

$$S_s = \left(\prod_1^N I_{js} L_j \right) I_{N+1s}, \quad S_p = \left(\prod_1^N I_{jp} L_j \right) I_{N+1p}, \quad (4)$$

where N is the layer number. The amplitude of reflectivity (r) is:

$$r_s = S_{21s} / S_{11s}, \quad r_p = S_{21p} / S_{11p}. \quad (5)$$

Final reflectance (R) is calculated as:

$$R_s = r_s r_s^*, \quad R_p = r_p r_p^*. \quad (6)$$

References

Andersson, S. (1999). Morphology of UV reflectance in a whistling-thrush: implications for the study of structural colour signalling in birds. *J. Avian Biol.* **30**, 193-204.

Borgia, G. (1986). Sexual selection in bowerbirds. *Sci. Am.* **254**, 92-100.

Brink, D. J. and van der Berg, N. G. (2004). Structural colours from the feather of the bird *Bostrychia hagedash*. *J. Phys. D Appl. Phys.* **37**, 813-818.

Cuthill, I. C., Bennett, A. T. D., Partridge, J. C. and Maier, E. J. (1999). Plumage reflectance and the objective assessment of avian sexual dichromatism. *Am. Nat.* **160**, 183-200.

Cuthill, I. C., Partridge, J. C., Bennett, A. T. D., Church, S. C., Hart, N. S. and Hunt, S. (2000). Ultraviolet vision in birds. *Adv. Stud. Behav.* **29**, 159-214.

Doucet, S. M. (2002). Structural plumage coloration, male body size, and condition in the Blue-Black Grassquit. *Condor* **104**, 30-38.

Doucet, S. M. and Montgomerie, R. (2003a). Bower location and orientation in Satin Bowerbirds: optimising the conspicuousness of male display? *Emu* **103**, 105-109.

Doucet, S. M. and Montgomerie, R. (2003b). Multiple sexual ornaments in satin bowerbirds: ultraviolet plumage and bowers signal different aspects of male quality. *Behav. Ecol.* **14**, 503-509.

Doucet, S. M. and Montgomerie, R. (2003c). Structural plumage colour and parasites in satin bowerbirds *Ptilonorhynchus violaceus*: implications for sexual selection. *J. Avian Biol.* **34**, 237-242.

Doucet, S. M., Shawkey, M. D., Rathburn, M. K., Mays, H. L. J. and Montgomerie, R. (2004). Concordant evolution of plumage colour, feather microstructure, and a melanocortin receptor gene between mainland and island populations of a fairy-wren. *Proc. R. Soc. Lond. B* **271**, 1663-1670.

Durrer, H. (1986). The skin of birds: colouration. In *Biology of the Integument*

2, Vertebrates (ed. J. Bereiter-Hahn A. G. Matolsky and K. S. Richards), pp. 239-247. Berlin: Springer-Verlag.

Dyck, J. (1978). Olive green feathers: reflection of light from the rami and their structure. *Anser* **3**, S57-S75.

Fitzpatrick, S. (1998). Colour schemes for birds: structural coloration and signals of quality in feathers. *Ann. Zool. Fenn.* **35**, 67-77.

Fox, D. L. (1976). *Animal Biochromes and Structural Colours*. Berkeley: University of California Press.

Greenwalt, C. H., Brandt, W. and Friel, D. (1960). The iridescent colors of hummingbird feathers. *J. Opt. Soc. Am.* **50**, 1005-1013.

Hailman, J. P. (1977). *Optical Signals: Animal Communication and Light*. Bloomington: Indiana University Press.

Hart, N. S. (2001). The visual ecology of avian photoreceptors. *Progr. Retin. Eye Res.* **20**, 675-703.

Hill, G. E., Doucet, S. M. and Buchholz, R. (2005). The effect of coccidial infection on iridescent plumage coloration in wild turkeys. *Anim. Behav.* **69**, 387-394.

Jellison, G. E., Jr (1993). Data analysis for spectroscopic ellipsometry. *Thin Solid Films* **234**, 416-422.

Keyser, A. J. and Hill, G. E. (1999). Condition-dependent variation in the blue-ultraviolet coloration of a structurally based plumage ornament. *Proc. R. Soc. Lond. B* **266**, 771-777.

Land, M. F. (1972). The physics and biology of animal reflectors. *Prog. Biophys. Mol. Biol.* **24**, 77-106.

McGraw, K. J., Mackillop, E. A., Dale, J. and Hauber, M. E. (2002). Different colors reveal different information: how nutritional stress affects the expression of melanin- and structurally based ornamental plumage. *J. Exp. Biol.* **205**, 3747-3755.

Montgomerie, R. (2006). Analyzing colors. In *Bird Coloration. Vol. 1. Mechanisms and Measurements* (ed. G. E. Hill and K. J. McGraw). Cambridge: Harvard University Press.

Newton, I. (1730). *Opticks*. 4th Edn. New York: Dover.

Osorio, D. and Ham, A. D. (2002). Spectral reflectance and directional properties of structural coloration in bird plumage. *J. Exp. Biol.* **205**, 2017-2027.

Prum, R. O. (1999). The anatomy and physics of avian structural colours. In *Proceedings of the 22nd International Ornithological Congress* (ed. N. J. Adams and R. H. Slotow), pp. 1633-1653. Durban: Bird Life South Africa.

Prum, R. O. (2006). Anatomy, physics, and evolution of avian structural colors. In *Bird Coloration. Vol 1. Mechanisms and Measurements* (ed. G. E. Hill and K. J. McGraw), pp. 295-355. Cambridge: Harvard University Press.

Prum, R. O., Torres, R., Williamson, S. and Dyck, J. (1998). Constructive interference of light by blue feather barbs. *Nature* **396**, 28-29.

Prum, R. O., Torres, R., Williamson, S. and Dyck, J. (1999). Two-dimensional Fourier analysis of the spongy medullary keratin of structurally coloured feather barbs. *Proc. R. Soc. Lond. B* **266**, 13-22.

Prum, R. O., Andersson, S. and Torres, R. H. (2003). Coherent scattering of ultraviolet light by avian feather barbs. *Auk* **120**, 163-170.

Shawkey, M. D., Estes, A. M., Siefferman, L. M. and Hill, G. E. (2003). Nanostructure predicts intraspecific variation in ultraviolet-blue plumage colours. *Proc. R. Soc. Lond. B* **270**, 1455-1460.

Shawkey, M. D. and Hill, G. E. (2005). Carotenoids need structural colours to shine. *Biol. Lett.* **1**, 121-124.

Vačíšek, A. (1960). *Optics of Thin Films*. Amsterdam: North Holland Publishing Company.

Vellenga, R. E. (1980). Moults of the satin bowerbird *Ptilonorhynchus violaceus*. *Emu* **80**, 49-54.

Zi, J., Yu, X., Li, Y., Hu, S., Xu, C., Wang, X., Liu, X. and Fu, R. (2003). Coloration strategies in peacock feathers. *Proc. Natl. Acad. Sci. USA* **100**, 12576-12578.